Asociación Argentina de Mecánica Computacional

Mecánica Computacional Vol XXVI, pp.2919-2930
Sergio A. Elaskar, Elvio A. Pilotta, Germán A. Torres (Eds.)
Córdoba, Argentina, Octubre 2007

SYNTHESIS OF COMPLIANT MECHANISMS FOR SEGMENT-MOTION GENERATION TASKS

Alejandro E. Albanesi, Victor D. Fachinotti, Martín A. Pucheta and Alberto Cardona

Centro Internacional de Métodos Computacionales en Ingeniería (CIMEC)
INTEC - Universidad Nacional del Litoral
Guemes 3450, 3000 Santa Fe, Argentina
aalbanes@ceride.gov.ar, http://www.cimec.org.ar

Keywords: Synthesis, Compliant Mechanisms.

Abstract. In mechanisms design, one of the more common tasks in kinematic synthesis is motion generation (rigid-body guidance), where a rigid body is moved through a specified motion. If the body to be guided is flexible and has an initial smooth shape, the task of moving it from its initial configuration to a specified, also smooth, configuration, is referred to as segment-motion generation. This is the case for compliant four-bar mechanisms, where the flexible coupler link is the body to be guided, and the (also flexible) input and follower links are the ones to be synthesized. Previous works on this type of compliant mechanism neglected the shear stress induced in the links, and the used technique disjoined the mechanism in order to synthesize a single-link at a time, that would accomplish the specified task. In this paper we conceive a more realistic approach, considering all flexible links as two dimensional beams with shear deformation, and synthesized the input and follower links simultaneously, as the flexible guided body is moved through a sequence of discrete prescribed "precision shapes" in addition to rigid-body motion, in order to achieve its specified task. The synthesis problem is solved by optimization of the finite element model, and the method is tested with a numerical example.

1 INTRODUCTION

Traditional rigid-body mechanisms consist of rigid links connected at movable joints, and their motion depend on rigid-body translations and/or rotations. Nowadays, many mechanisms are designed to derive some mobility by elastic deformation in one or more elements, that is, they gain at least some of their mobility from the deflection of flexible members rather than from movable joints only. This latter group is widely known as *compliant mechanisms*.

Kinematic synthesis is the means used to design mechanisms for a specified motion (see Erdman and Sandor, 1997). Three of its common tasks are function, path and motion generation. In this work we will consider *motion generation* (also known as rigid-body guidance), where a rigid body is moved trough a specified motion. This prescribed rigid-body motion sequence comprises the desired positions and orientations of the link. The functions, path and motion specified cannot, in general, be generated exactly for the entire mechanism motion, but they may be specified and met at a certain number of points called *precision points*.

We shall focus our work on a four-bar mechanism, wich is a closed-loop kinematic chain. One of the links is called the *coupler link*, and is the only one that can trace paths of arbitrary shape because it is not rotating about a fixed pivot. Previous research on this type of mechanisms comprised at least one moving rigid link, and the coupler-link was always considered a rigid member, because the motion generation objective is based on the task definition for conventional rigid-link mechanisms. In this paper we consider a *compliant four-bar mechanism*, because all its motion is obtained from the deflection of compliant members. The bars are modeled as beams with shear deformation, thus involving the guidance of a flexible link rather than a rigid body. This implies moving the *compliant coupler-link* through a sequence of discrete prescribed *precision shapes* in addition to the precision points in rigid-body motion.

Saggere and Kota (2001) presented this problem and called the task of accomplishing such motion *compliant-segment motion generation*. In order to synthesize the flexible links, they used a technique called *pseudo-rigid-body model* developed by Howell and Midha (1996), and Howell (2001), where a compliant mechanism is modeled as an equivalent rigid-link mechanism, to synthesize a fully-compliant four-bar mechanism. The purpose of the pseudo-rigid-body model is to provide a simple method of analyzing systems that undergo large, nonlinear deflections, where flexible members are modeled as rigid links attached at pin joints. Despite the fact that torsional springs are added to account the force-deflection relationship, this method does not account for the shear stress and/or force that may appear in the links as they deflect from their initial to final configuration.

In this paper we conceived a more realistic approach, and modeled all compliant links using a two-dimensional finite element formulation for the beam with shear deformation, and a general procedure to synthesize a compliant, single-loop mechanism. The extension of this work to synthesize multi-loop mechanisms can be easily arranged.

Many potential applications of compliant-segment motion generation can be envisioned. For instance, a certain segment of a large flexible space structure that functions as a reflective surface may be required to be oriented in different directions and also shaped into different curvatures for the purposes of modulating the characteristics of reflecting sound or light waves. A similar application of compliant-segment motion generation is also practicable at micro level, for example, in micromirrors for controlled reflection of light. Another example of potential application of compliant-segment motion generation is a stamping application where a flexible contour is required to conform to contoured rigid surfaces that have differently shaped curvatures. In all such applications, the required task can be efficiently accomplished by devising a suitable compliant four-bar mechanism.

2 PROBLEM DESCRIPTION

As mentioned above, given a four-bar mechanism, only the *coupler link* is able to trace paths of arbitrary shape, because it does not rotate about a fixed pivot. One of the grounded links serves as the *input or driver link*, which may either be turned by hand or perhaps driven by an electric motor or a hydraulic or pneumatic cylinder. The remaining grounded link is called the *follower or driven link*, because its rotation merely follows the motion as determined by the input and coupler link motion. This is shown in Figure 1.

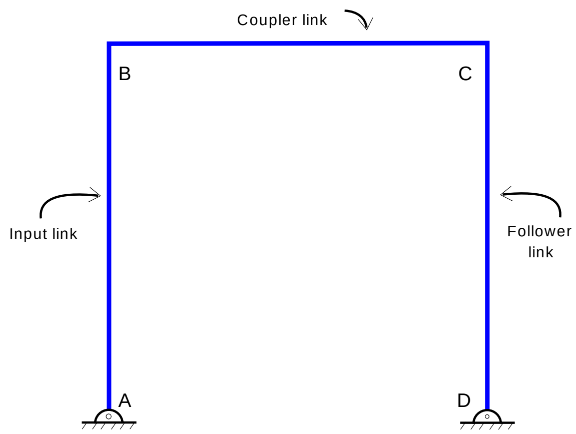

Figure 1: A four-bar mechanism

The objective of the synthesis is to guide a given flexible segment (the coupler link) with initial, smooth configuration to a specified, also smooth, final configuration as shown in Figure 2. This motion from initial to final configuration of the flexible segment is in fact the *mechanism task*.

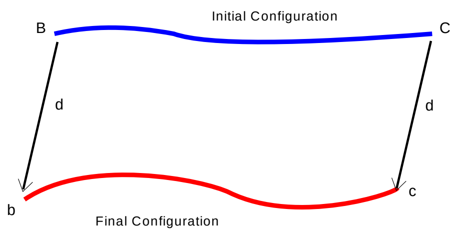

Figure 2: Mechanism task: the guided, flexible coupler-link

The two ends of the compliant coupler-link are connected to the ends of the compliant input and follower links (the ones to be synthesized), and the three segments form one continuous planar link. The minimum number of variables required to describe the configuration of a mechanism completely is called its *degrees of freedom*. An unconstrained planar link has three degrees of freedom, because three displacements variables are required to describe its position and orientation (two displacements, one in the x coordinate and the other in the y coordinate, and one rotation around an axis perpendicular to the xy plane). A *lower kinematic pair*, such as a revolute joint or *hinge*, removes two degrees of freedom, allowing only rotations about the hinged end. If a planar link is *clamped*, all its degrees of freedom are removed. The free end the follower link may either be pinned or clamped to the ground. The input link can only be *pinned* to the ground if the mechanism is to be actuated from that point by an input torque or rotation, as shown in Figure 3. In this figure, B-C is the given flexible segment to be guided to a specified final configuration b-c; A-B and C-D are two segments to be synthesized; A-B-C-D represents the initial configuration and A-b-c-D the final configuration of the mechanism.

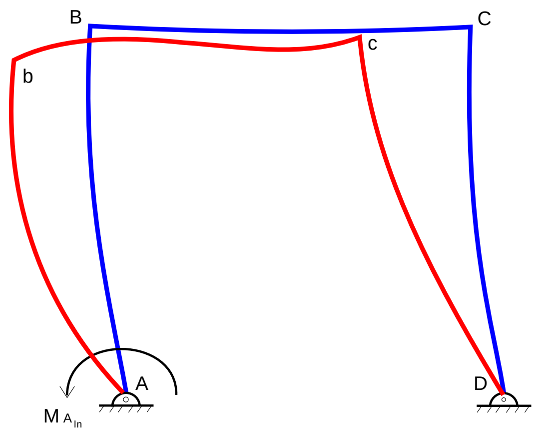

Figure 3: Specified initial and final configuration of the mechanism

According to this, a more formal definition of the problem can be stated: *given a compliant segment and its initial and final desired configuration, synthesize the input and follower links of a compliant four-bar mechanism and the corresponding input torques and/or rotations, that precisely induce the prescribed compliant-segment motion generation.*

3 SYNTHESIS PROCEDURE

The synthesis tasks are to determine: optimal shapes and sizes of segments A-B and C-D, locations of the pivots A and D, and the input torque and/or rotation in pivot A, so that the coupler link may be guided from its initial to the final desired configuration. The matrix assembly in the finite element formulation used allowed us to synthesize the mechanism as a closed-loop kinematic chain, and simultaneously guarantee the equilibrium of the mechanism and that all links are, effectively joined.

This is a somewhat different approach than the one adopted for rigid-link four-bar mechanisms, which involves disjoining the mechanism into various links and designing each link separately, imposing boundary conditions on each segment in order to accomplish identical displacements and rotations at the fusing ends, in which case the internal forces and moments are equal in magnitude but opposite in sign, and therefore all segments are independently in equilibrium.

3.1 Finite Element Formulation

It was mentioned before that the pseudo-rigid body model neglects the shear stress and/or force that could be induced in the compliant links as they deflect, in order for a compliant mechanism to undergo any amount of motion. Instead, we decided to use two-dimensional finite element formulation, adopting Timoshenko's beam formulation, which includes shear deformation. The following formulation was derived by Crisfield (1991), and it assumes the hypothesis that *plane sections, normal to the axis of the beam, remain plain but not necessarily normal to the axis after deflection*. A very similar formulation was derived by Omar et al. (2000).

We use an initially curved element as shown in Figure 4 (this element can also be used if the beam is initially straight). By assuming plane sections remain plane, the displacement in the x direction, u, at distance z, from the centroid is given (see Figure 5) by

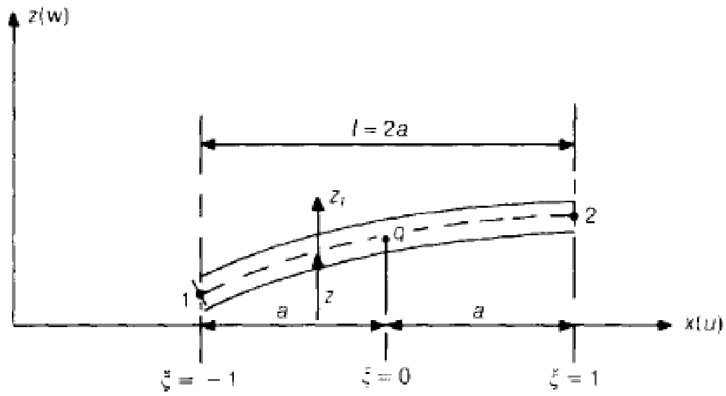

Figure 4: Initially curved beam element

$$u = \overline{u} + z_l \frac{d\theta}{dx} \tag{1}$$

θ is the rotation of the normal of the beam, and it can be expressed as

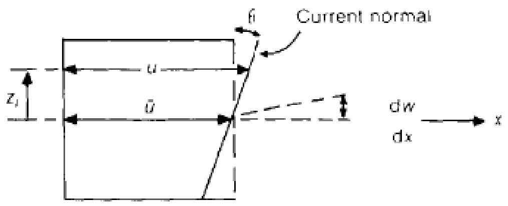

Figure 5: Detail of the beam element with shear deformation

$$\theta = \frac{dw}{dx} + \phi \tag{2}$$

where ϕ is the additional rotation induced by the shear strains (see Oñate, 1992). The curvature, χ, is defined as

$$\chi = \frac{d\theta}{dx} \tag{3}$$

The axial strain in the x direction can, using a degenerated form of the Green strain, be expressed as

$$\varepsilon_x = \frac{d\overline{u}}{dx} + \frac{1}{2}\left(\left(\frac{d\left(z+w\right)}{dx}\right)^2 - \left(\frac{dz}{dx}\right)^2\right) + z_l\chi = \overline{\varepsilon} + z_l\chi \tag{4}$$

The virtual work equation can be expressed as

$$V = \int \left(N\left(\frac{d\delta\overline{u_v}}{dx} + \frac{dw'}{dx}\frac{d\delta w_v}{dx}\right) + M\delta\chi_v + Q\left(\delta\theta_v + \frac{d\delta w_v}{dx}\right)\right) dx - \boldsymbol{q_e^T \delta p_v} \tag{5}$$

where $\boldsymbol{q_e}$ is the load vector at the end node and $\boldsymbol{p_v}$ is the vector of virtual nodal displacements.

By assuming elastic properties, the normal force N, the moment M, and the transverse shear force Q, are defined in (5) as

$$N = EA\overline{\varepsilon} \qquad M = EI\chi \qquad Q = GA\gamma \tag{6}$$

In addition, the displacement in the x direction u, the displacement in the z direction w, and the rotation of the normal θ, will be expressed as

$$\boldsymbol{u} = (u_1, u_2, \Delta u_q) \qquad \boldsymbol{w} = (w_1, w_2, \Delta w_q) \qquad \boldsymbol{\theta} = (\theta_1, \theta_2, \Delta\theta_q) \tag{7}$$

where the suffix 1 refers to the first node and the suffix 2 refers to the second node of the element.

At this stage, the finite element shape functions can be introduced. We will adopt quadratic hierarchical functions for u, w and θ, so that

$$\overline{u} = \boldsymbol{h_u^T u} \qquad w = \boldsymbol{h_w^T w} \qquad \theta = \boldsymbol{h_\theta^T \theta} \tag{8}$$

where the functions $\boldsymbol{h_u} = \boldsymbol{h_w} = \boldsymbol{h_\theta}$ are given by equation

$$\boldsymbol{h_u^T u} = \frac{1}{2}\left(1-\xi, 1+\xi, 2\left(1-\xi^2\right)\right) \tag{9}$$

With a view to the computation of the strains, differentiation of (9) leads to

$$\frac{d\overline{u}}{dx} = \frac{1}{l}\left(-1, 1, -4\xi\right)\boldsymbol{u} = \boldsymbol{b_u^T u} \tag{10}$$

Exactly in the same way,

$$\frac{dw}{dx} = \boldsymbol{b_w^T w} \qquad \frac{d\theta}{dx} = \boldsymbol{b_\theta^T \theta} \tag{11}$$

where once again $\boldsymbol{b_u} = \boldsymbol{b_w} = \boldsymbol{b_\theta}$.

Since equation (4) can be expressed as

$$\overline{\varepsilon} = \boldsymbol{b_u^T u} + \frac{1}{2}\left(\boldsymbol{b_w^T w'}\right)^2 - \frac{1}{2}\left(\boldsymbol{b_w^T z}\right)^2 \tag{12}$$

and using equation (11), the shear strain and the curvature are given by

$$\gamma = \theta + \frac{dw}{dx} = \boldsymbol{b_w^T w} + \boldsymbol{h_\theta^T \theta} \qquad \chi = \frac{d\theta}{dx} = \boldsymbol{b_\theta \theta} \tag{13}$$

Consequently, from (5), the internal virtual work becomes

$$V_i = \int N\left(b_u^T \delta u_v + \left(b_w^T w'\right) b_w^T \delta w_v + M b_\theta^T \delta\theta_v + Q\left(h_\theta^T \delta\theta_v + b_w^T \delta w_v\right)\right) dx \tag{14}$$

and the internal force vector is

$$\boldsymbol{q_i^T} = \left(\boldsymbol{U_i^T}, \boldsymbol{W_i^T}, \boldsymbol{T_i^T}\right) \tag{15}$$

where the T_i terms are work-conjugate to the nodal rotations, θ. The components of q_i are given by

$$\boldsymbol{U_i} = \int N\boldsymbol{b_u} dx \tag{16}$$

$$\boldsymbol{W_i} = \int \left(N\left(\boldsymbol{b_w^T w'}\right) b_w + Q\boldsymbol{b_w}\right) dx \tag{17}$$

$$\boldsymbol{T_i} = \int \left(M\boldsymbol{b_\theta} + Q\boldsymbol{h_\theta}\right) dx \tag{18}$$

The tangent stiffness matrix is obtained in the usual manner by differentiation of the internal force vector. To this end, it is most convenient to subdivide the tangent stiffness matrix in submatrices, so that

$$\mathbf{K_t} = \begin{pmatrix} K_{uu} & K_{uw} & K_{u\theta} \\ K_{uw}^T & K_{ww} & K_{w\theta} \\ K_{u\theta}^T & K_{w\theta}^T & K_{\theta\theta} \end{pmatrix} = \begin{pmatrix} \frac{\partial U_i}{\partial u} & \frac{\partial U_i}{\partial w} & \frac{\partial U_i}{\partial \theta} \\ \frac{\partial W_i}{\partial u} & \frac{\partial W_i}{\partial w} & \frac{\partial W_i}{\partial \theta} \\ \frac{\partial \theta_i}{\partial u} & \frac{\partial \theta_i}{\partial w} & \frac{\partial \theta_i}{\partial \theta} \end{pmatrix} \tag{19}$$

where from (16), (17) and (18) the submatrices are given by

$$\boldsymbol{K_{uu}} = \int EA\boldsymbol{b_u b_u^T} dx \tag{20}$$

$$\boldsymbol{K_{uw}} = \int EA\left(\boldsymbol{b_w^T w'}\right)\boldsymbol{b_u b_w^T} dx \tag{21}$$

$$\boldsymbol{K_{u\theta}} = 0 \tag{22}$$

$$\boldsymbol{K_{ww}} = \int \left(EA\left(\boldsymbol{b_w^T w'}\right)^2 \boldsymbol{b_w b_w^T} + GA\boldsymbol{b_w b_w^T} + N\boldsymbol{b_w b_w^T}\right) dx \tag{23}$$

$$\boldsymbol{K_{w\theta}} = \int GA\boldsymbol{b_w h_\theta} dx \tag{24}$$

$$\boldsymbol{K_{\theta\theta}} = \int EI\left(\boldsymbol{b_\theta b_\theta^T} + GA\boldsymbol{h_\theta h_\theta^T}\right) dx \tag{25}$$

The term $N\boldsymbol{b_w b_w^T}$, in (23), is the *initial stress* or *geometric* stiffness matrix. In (23) - (25), the GA terms should include a shape-function factor for shear ($\frac{5}{6}$ for a rectangular section).

3.2 Synthesis of the Input and Follower Segments

The most common problem in the theory of bending, is when the unloaded shape of a beam is given, and the loaded shape is sought. This problem is rather straight-forward to solve. There also exist problems that are the inverse of this direct bending problem. For instance, the deflected (loaded) shape of a beam is given and the loads are known, in which case the free unloaded the equilibrium-shape is sought (see for example Fachinotti et al., 2005).

The inverse problem we are dealing with, is such that both, *the initial and loaded shapes of the compliant input and follower links are not known, nor are the tip locations and length of the segment known*. However, the tip loads, displacements and rotations are known. All these inverse problems have, in general, no closed form solutions, and they require numerical methods in order to be solved.

In our scheme, the synthesis process of the compliant input and follower links were carried out using an optimization scheme. The first step comprises setting up the right boundary conditions on the three segments. These boundary conditions are derived from the specified mechanism task. Once they are established, the optimization process is started in order to *determine the shapes and sizes of segments A-B and C-D, the locations of the pivots A and D, and the unknown input torque and/or rotation in pivot A; so that when it is applied to the recently synthesized mechanism, its motion agrees with its specified task.*

The motion of the compliant coupler link is determined by its known initial configuration (geometry and shape) and also known final configuration (specified mechanism task). This change in curvature (motion) is translated into displacements and rotations at pivots B and C. The forces and moments induced by this motion are directly calculated by the finite element formulation. Five finite elements per link are used ($i = 1...n$, where $n = 5$). Afterwards, the optimization (synthesis) process is started. All classical optimization algorithms solve the same mathematical problem: minimize a given *objective function* f (if by minimizing f we obtain a better design), subject to one or more *constraints* by variation of the *design variables* between prescribed values (see Vanderplaats, 1984).

The objective function is the volume of the compliant input and follower links, which has to be minimized. The design variables are given by: the length of the link H, the cross-section width b, the cross-section height h, the position angle α and rotation angle θ. The constraints are the displacements and rotations given by the specified mechanism task, and are represented by u (displacement in the x direction), w (displacement in the z direction), and the rotation angle by θ. The mechanism task is the function $t(x, w, \theta)$ and $\bar{t}$ is the specified task. From now on, the suffix 1 refers to the input and the suffix 2 to the follower link. A weight factor (penalization) is added in order to assure that these displacements and rotations are matched. Thus, the optimization problem can be stated as follows:

Minimize: Volume

$$f = min(\sum_{i=1}^{n}(H_i b_i h_i)) \tag{26}$$

Subject to: Mechanism Task

$$t(x, w, \theta) = \bar{t} \tag{27}$$

Modifying: Design Variables

$$X = [H_1, H_2, b_1, b_2, h_1, h_2, \alpha_1, \alpha_2, \theta_1] \tag{28}$$

In other words, *we are trying to satisfy the specified mechanism task, using the minimum amount of material.*

4 NUMERICAL EXAMPLE

In what follows, we are going to compare the results obtained with our model with the reference results obtained by Saggere and Kota (2001). Consider a rectangular flexible beam which is initially straight, and it is required to be guided and deformed, to a new specified configuration (the imposed, initially straight, shape of the beam is simply assumed in order to make a coherent comparison with the aformencioned reference results).

The beam is $L = 200$ mm long, the cross sectional height is $h = 5$ mm and the cross sectional width is $b = 5$ mm. As shown in Figure 6, α is the initial position angle, and θ the

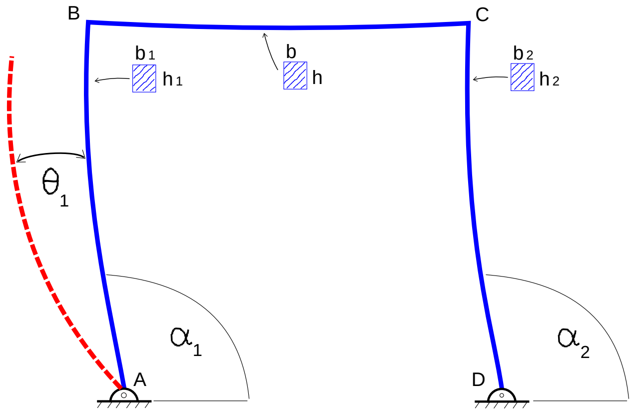

Figure 6: Details for some of the design variables

input segment rotation angle. The material properties are: Young modulus $E = 2 \times 10^5$ N/mm^2 and shear modulus $G = 8.33 \times 10^4$ N/mm^2.

Let the required displacements at the two free ends be $d = 10$ mm at an angle $\beta = 5.53^o$. The rotations at the ends of the flexible coupler link are computed from the known change in geometry: $\theta_B = -0.1$ rad and $\theta_C = -0.08$ rad. No external load is applied. This can be seen in Figure 7.

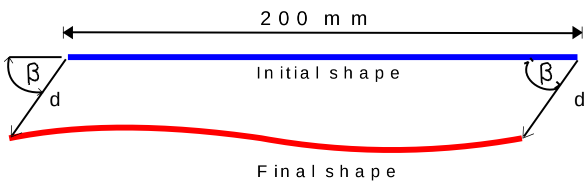

Figure 7: Specified task for the compliant coupler-link

Next, the compliant input and follower links are synthesized using the optimization scheme described above. In the first example, the grounded ends of these segments are hinged to the ground (both ends are lower kinematic pairs). The optimization problem was setup and solved in *fmincon*, the optimization module in the MATLAB software package.

The chosen bounds for the design variables are shown in Table 1:

Var	H_1	H_2	b_1	b_2	h_1	h_2	α_1	α_2	θ_1
Min	10	10	5	5	5	5	0.1 π	0.1 π	-0.4 π
Max	120	120	50	50	50	50	0.9 π	0.9 π	0.4 π

Table 1: Bounds for the design variables.

4.1 Both free ends hinged to the grounds

The results for both free ends hinged to the ground are shown in Table 2 (the units are: for linear dimension mm, for moments Nmm, and for rotations in radians):

The maximum constraint error for this model is below $e_R\ le 1\%$. As we can see in Figure 8, the length of the follower segment is somewhat longer than the length of the input link, and their

Var	H_1	H_2	b_1	b_2	h_1	h_2	α_1	α_2	θ_1	M_A
Value	62.49	73.63	5.10	5.18	6.13	5.13	1.58	1.60	-0.23	-52697.9

Table 2: Results for both free ends hinged to the ground.

curvature is very small, as it can be expected in hinged segments. The volume of material used is $V = 8910.2$ mm^3, 65% less than the value obtained by Saggere and Kota (2001) for the same boundary conditions (their value is $V = 25509$ mm^3. The same mechanism task is achieved, *using much less than halve the volume*. This is summarized in Table 3.

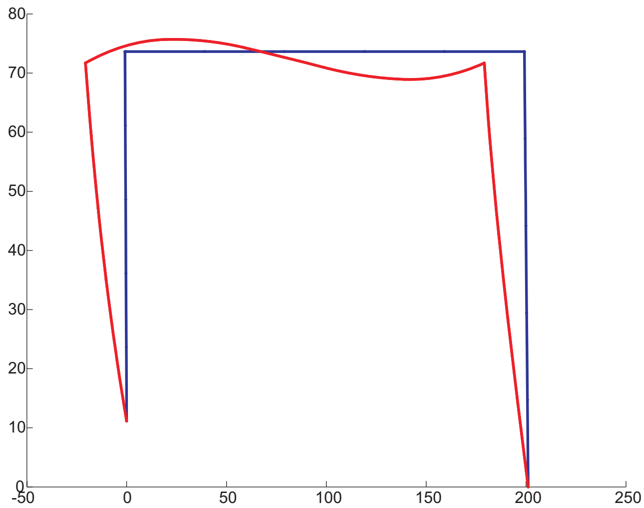

Figure 8: Results for both free ends hinged to the ground

Model	Proposed	Saggere et al.
Boundary	Hinged-Hinged	Hinged-Hinged
Total Volume	8910.2 mm^3	25509 mm^3
Relative Volume	35%	100%
Material Saved	65%	—

Table 3: Volume of material used for the mechanism.

4.2 One free end hinged and the other clamped to the ground

It is of some interest to verify how the mechanism changes its topology when the free end of the follower link is clamped. The maximum constraint error for this model is below $e_R \leq 1.5\%$. The results for this particular boundary condition are shown in Table 4 (once again, the units are: for linear dimension mm, for moments Nmm, and for rotations in radians).

As it was expected, the length of the follower link should increase, in order to gain the flexibility needed for the mechanism task, this can be seen in Figure 9.

The volume of material used is $V = 12306$ mm^3. Even for this boundary condition (worst than the hinged-hinged condition, because extra length of the follower link is obtained), the volume is 51% lower than the volume obtained by Saggere and Kota (2001), while the same mechanism task is achieved. This is summarized in Table 5.

Var	H_1	H_2	b_1	b_2	h_1	h_2	α_1	α_2	θ_1	M_A
Value	63.66	115.37	6.86	7.99	6.07	5.05	1.58	1.61	-0.24	-75499.1

Table 4: Results for one end hinged and the other clamped to the ground.

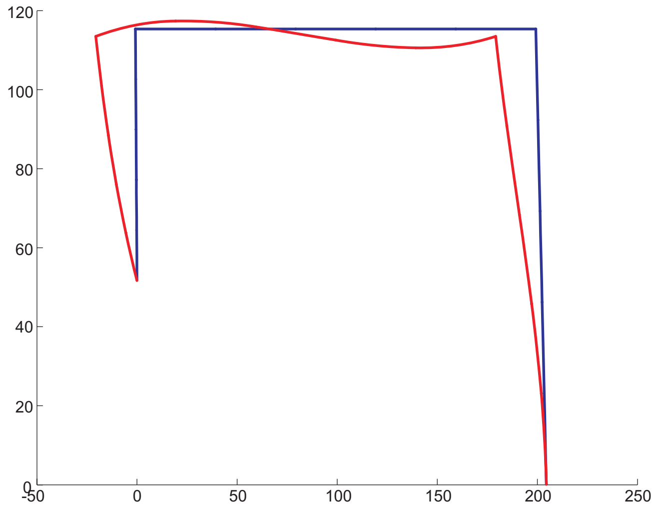

Figure 9: Results for one end hinged and the other clamped to the ground

5 CONCLUSIONS

The present work introduces a more realistic approach for compliant-segment motion generation tasks, where a flexible body is moved through a sequence of prescribed shapes in addition to the prescribed points in rigid-body motion.

The pseudo-rigid body model is replaced by a two-dimensional finite element formulation for the beam with shear deformation. The extra shear-strain that may be induced in the links as they deflect from their initial to final configuration is now quantified, and this becomes particularly useful when the mechanism to be studied is not slender. Thus, this formulation allows to synthesize the input and follower links simultaneously, as the flexible guided body is moved according to the specified mechanism task.

This procedure is shown in a numerical example, and two different boundary conditions are analyzed. The results obtained demonstrated the feasibility of the method, and less material is needed in order to accomplish the specified mechanism task. The extension of this work to synthesize multi-loop mechanisms can be easily arranged.

Currently, improvement of the model by adding large-non linear deflections is in progress.

ACKNOWLEDGEMENTS

The authors gratefully acknowledge the financial support from the Consejo Nacional de Investigaciones Científicas y Técnicas (CONICET).

Model	Proposed	Saggere et al.
Boundary	Hinged-Clamped	Hinged-Hinged
Total Volume	12306 mm^3	25509 mm^3
Relative Volume	49%	100%
Material Saved	51%	—-

Table 5: Volume of material used for the mechanism.

REFERENCES

Crisfield M. A. Non-linear Finite Element Analysis of Solids and Structures, Volume 1. John Wiley & Sons, 1991.

Erdman A. G., Sandor G. N., Mechanism Design: Analysis and Synthesis, 3rd Edition, Prentice-Hall, 1997.

Fachinotti V. D., Cardona A., and Jetteur P. Finite Element Modelling of Inverse Design Problems in Large Deformations Anisotropic Hyperelasticity, *International Journal for Numerical Methods in Engineering*, 2005.

Howell L. L. Compliant Mechanisms, John Wiley & Sons, 2001.

Howell L. L., and Midha A. A Loop-Closure Theory for the Analysis and Synthesis of Compliant Mechanisms, *ASME Journal of Mechanical Design*, Vol 118, No. 1, pp. 121-125, 1996.

Omar M. A., and Shabana A. A. A Two-Dimensional Shear Deformable Beam For Large Rotations and Deformation Problems, *Journal of Sound and Vibration*, Vol 243, No. 3, pp. 565-576, 2000.

Oñate E. Cálculo de Estructuras por el Método de Elementos Finitos. CIMNE. 1992.

Saggere L., and Kota S. Synthesis of Planar, Compliant Four-Bar Mechanisms for Compliant-Segment Motion Generation, *ASME Journal of Mechanical Design*, Vol. 123, pp. 535-541, (2001).

Vanderplaats G. Numerical Optimization Techniques for Engineering Design, McGraw-Hill, 1984.